Article

An Osmium–DNA Interstrand Complex: Application to Facile DNA Methylation Analysis

Kazuo Tanaka, Kazuki Tainaka, Tadashi Umemoto, Akiko Nomura, and Akimitsu Okamoto

J. Am. Chem. Soc., **2007**, 129 (46), 14511-14517• DOI: 10.1021/ja076140r • Publication Date (Web): 27 October 2007

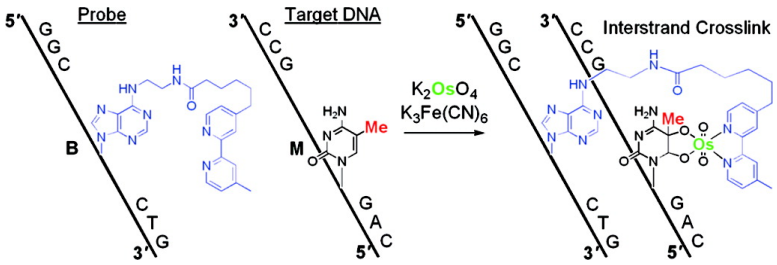

More About This Article

Additional resources and features associated with this article are available within the HTML version:

- Supporting Information
- Links to the 4 articles that cite this article, as of the time of this article download
- Access to high resolution figures
- Links to articles and content related to this article
- Copyright permission to reproduce figures and/or text from this article

View the Full Text HTML

J|A|C|S
ARTICLES
Published on Web 10/27/2007

An Osmium−DNA Interstrand Complex: Application to Facile DNA Methylation Analysis

Kazuo Tanaka, Kazuki Tainaka, Tadashi Umemoto, Akiko Nomura, and Akimitsu Okamoto*

Contribution from the Frontier Research System, RIKEN (The Institute of Physical and Chemical Research), Wako, Saitama 351-1098, Japan

Received August 15, 2007; E-mail: aki-okamoto@riken.jp

Abstract: Nucleic acids often acquire new functions by forming a variety of complexes with metal ions. Osmium, in an oxidized state, also reacts with C5-methylated pyrimidines. However, control of the sequence specificity of osmium complexation with DNA is still immature, and the value of the resulting complexes is unknown. We have designed a bipyridine-attached adenine derivative for sequence-specific osmium complexation. Sequence-specific osmium complexation was achieved by hybridization of a short DNA molecule containing this functional nucleotide to a target DNA sequence and resulted in the formation of a cross-linked structure. The interstrand cross-link clearly distinguished methylated cytosines from unmethylated cytosines and was used to quantify the degree of methylation at a specific cytosine in the genome.

Introduction

Metal complexes are involved in modulating the variety of structures and functions of nucleic acids and labeling of nucleic acids in many scientific studies.[1] For example, ribozymes have divalent metal ions such as magnesium and cadmium ions as cofactors.[2] Platinum(II) complexes are known to form complexes with guanine bases in DNA.[3] Europium(III) and gadolinium(III) have been used for DNA labeling as red phosphors for fluorescence imaging and as a radiocontrast agent to enhance images in magnetic resonance imaging, respectively.[4] Osmium is a metallic element that is usually absent from cells, but its oxides are chemical reagents that oxidize carbon−carbon double bonds to diols and are often used as a tissue stain. Osmium oxidation is used as a thymine-targeting sequencing technique,[5] and thymine bases are converted to thymine glycols by osmium tetroxide.[6] The combination of potassium osmate(VI), which is much less intractable than osmium tetroxide, with potassium hexacyanoferrate(III) as an activator and bipyridine as a reaction-accelerating ligand produces an osmium-centered complex with 5-methylcytosine (Scheme 1).[7] However, control of the sequence specificity of osmium oxidation of C5-methylated pyrimidines in DNA is still in its early stages, and thus the functional value of the resulting complexes is unclear. If the chemistry for sequence-specific, efficient osmium complexation at the target 5-methylcytosine is established, the resulting osmium complex would produce a conceptually new assay for DNA methylation analysis.

We herein report a new aspect of osmium−DNA complexation, applicable to a simple, sequence-specific, quantitative methylation analysis. We designed a bipyridine-attached adenine derivative for sequence-specific osmium complexation. Osmium complexation was achieved by hybridization of a short DNA molecule containing this functional nucleotide to a target DNA sequence, resulting in a sequence-specific cross-linked structure. The interstrand cross-link clearly distinguished methylated cytosines from unmethylated cytosines and was used to quantify the degree of methylation at a specific cytosine in the genome.

Results and Discussion

Osmium Complexation for a 5-Methylcytosine−Adenine-Mismatched Base Pair. We focused on the effects of the DNA

(1) (a) Richards, A. D.; Roger, A. *Chem. Soc. Rev.* **2007**, *36*, 471−483. (b) Boerner, L. J. K.; Zaleski, J. M. *Curr. Opin. Chem. Biol.* **2005**, *9*, 135−144. (c) Metcalfe, C.; Thomas, J. A. *Chem. Soc. Rev.* **2003**, *32*, 215−224.
(2) (a) Freisinger, E.; Sigel, R. K. O. *Coord. Chem. Rev.* **2007**, *251*, 1834−1851. (b) Fedor, M. J. *Curr. Opin. Struct. Biol.* **2002**, *12*, 289−295. (c) Narlikar, G. J.; Herschlag, D. *Annu. Rev. Biochem.* **1997**, *66*, 19−59. (d) Symons, R. H. *Crit. Rev. Plant Sci.* **1991**, *10*, 189−234.
(3) (a) Abu-Surrah, A. S.; Kettunen, M. *Curr. Med. Chem.* **2006**, *13*, 1337−1357. (b) van Zutphen, S.; Reedijk, J. *Coord. Chem. Rev.* **2005**, *249*, 2845−2853. (c) Wang, D.; Lippard, S. J. *Nat. Rev. Drug Discovery* **2005**, *4*, 307−320. (d) Zhang, C. X.; Lippard, S. J. *Curr. Opin. Chem. Biol.* **2003**, *7*, 481−489.
(4) (a) Hemmila, I.; Laitala, V. *J. Fluoresc.* **2005**, *15*, 529−542. (b) Horsey, I.; Krishnan-Ghosh, Y.; Balasubramanian, S. *Chem. Commun.* **2002**, 1950−1951. (c) Elbanowski, M.; Makowska, B. *J. Photochem. Photobiol. A* **1996**, *99*, 85−92. (d) Hurskainen, P.; Dahlen, P.; Ylikoski, J.; Kwiatkowski, M.; Siitari, H.; Lovgren, T. *Nucleic Acids Res.* **1991**, *19*, 1057−1061.
(5) (a) Palecek, E. *Methods Enzymol.* **1992**, *212*, 139−155. (b) Beer, M.; Stern, S.; Carmalt, D.; Mohlhenrich, K. H. *Biochemistry* **1966**, *5*, 2283−2288. (c) Nakatani, K.; Hagihara, S.; Sando, S.; Miyazaki, H.; Tanabe, K.; Saito, I. *J. Am. Chem. Soc.* **2000**, *122*, 6309−6310. (d) Ford, H.; Chang, C.-H.; Behrman, E. J. *J. Am. Chem. Soc.* **1981**, *103*, 7773−7779. (e) Ide, H.; Kow, Y. W.; Wallace, S. S. *Nucleic Acids Res.* **1985**, *13*, 8035−8052.
(6) (a) Vaishnav, Y.; Holwitt, E.; Swenberg, C.; Lee, H. C.; Kan, L. S. *J. Biomol. Struct. Dyn.* **1991**, *8*, 935−951. (b) Subbaraman, L.R.; Subbaraman, J.; Behrman, E. J. *Bioinorg. Chem.* **1971**, *1*, 35−55. (c) Chang, C.-H.; Ford, H.; Behrman, E. J. *Inorg. Chim. Acta* **1981**, *55*, 77−80. (d) Dizdaroglu, M.; Holwitt, E.; Hagan, M. P.; Blakely, W. F. *Biochem. J.* **1986**, *235*, 531−536.
(7) (a) Okamoto, A.; Tainaka, K.; Kamei, T. *Org. Biomol. Chem.* **2006**, *4*, 1638−1640. (b) Tanaka, K.; Tainaka, K.; Okamoto, A. *Bioorg. Med. Chem.* **2007**, *15*, 1615−1621. (c) Tanaka, K.; Tainaka, K.; Kamei, T.; Okamoto, A. *J. Am. Chem. Soc.* **2007**, *129*, 5612−5620.

Scheme 1. Osmium Complexation at 5-Methylcytosine

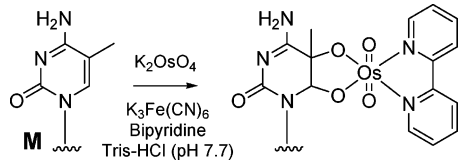

structure on osmium oxidation to sequence-specifically restrict the reactive pyrimidine. Cytosine−adenine-mismatched base pairs adopt a wobble-type structure with the cytosine displaced laterally into the major groove and the adenine into the minor groove by hydrogen bonding between the 6-amino group of adenine and the N3 of cytosine (Figure 1a).[8] Therefore, the formation of a cytosine−adenine-mismatched pair would cause partial disruption of π-stacking of the DNA duplex and facilitate oxidation at the C5−C6 double bond of the cytosine forced out of the DNA major groove. We prepared a short sequence containing a methylated/unmethylated cytosine, 5′-^{32}P-d(AAAAGAAGNGAGAAAA)-3′ (^{32}P-labeled DNA1(N), N = 5-methylcytosine (M) or C), and examined the reactivity of the single-stranded form, a fully matched helix, and a 5-methylcytosine−adenine-mismatched helix to osmium oxidation. ^{32}P-Labeled DNA1(N) and the strand to be hybridized, 5′-d(TTTTCTCN′CTTCTTTT-3′ (DNA1′(N′), N′ = G or A), were added to a mixture containing potassium osmate(VI), potassium hexacyanoferrate(III), and bipyridine, and the mixture was incubated at 0 °C for 5 min. The oxidized strand was cleaved at the damaged pyrimidine base with hot piperidine (90 °C, 20 min), and the products were analyzed as bands representing the shortened strands using polyacrylamide gel electrophoresis (PAGE, Figure 1b). Cleavage of the ^{32}P-labeled DNA1(C) was negligible, regardless of the nature of the base opposite cytosine (lanes 1, 3, and 5). The oxidation of bases in a fully Watson−Crick base-paired duplex was also strongly suppressed because of the protection of the C5−C6 double bond by the stacking of the flanking base pairs (lanes 3 and 4). The reaction of the duplex containing a 5-methylcytosine−adenine-mismatched base pair specifically proceeded at the 5-methylcytosine (lane 6), although the reaction rate was slightly lower than that observed for a single-stranded state (lane 2). Mass spectrometric analysis of the oxidation product obtained from a nonradiolabeled DNA1(M)/DNA1′(A) duplex showed that an osmium-centered complex, as shown in Scheme 1, was formed at the 5-methylcytosine of DNA1(M) ($[M + H]^+$, calcd 5085.60, found 5086.82). A 5-methylcytosine−adenine-mismatched base pair gave an osmium complex at 5-methylcytosine, different from the negligible reactivity of the full-matched duplex. On the basis of the osmium complexation reactivity of the 5-methylcytosine−adenine-mismatched base pair, the connection between an adenine base of a short DNA involved in a mismatched hybridization and the bipyridine ligand required for osmium-centered complex formation should result in complexation at a specific 5-methylcytosine, regardless of other reactive bases in a long DNA strand.

Design of a Functional Nucleoside for Sequence-Selective Osmium Complexation. We designed a functional nucleoside

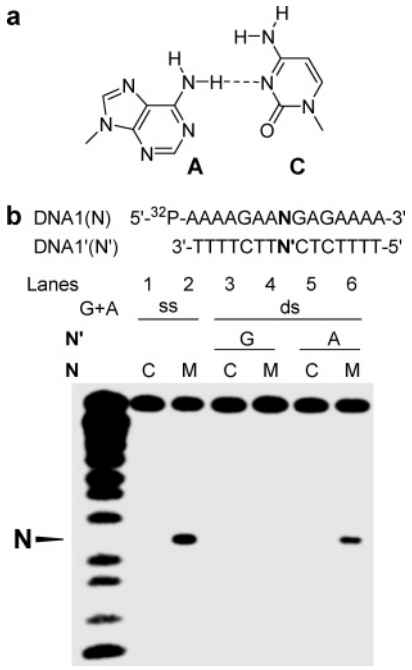

Figure 1. Osmium complexation at an adenine−5-methylcytosine-mismatched base pair. (a) An adenine−cytosine wobble base pair.[8] (b) Structural control of osmium complexation with a DNA strand containing an unmethylated (C) or methylated cytosine (M).

in which an adenine base and a bipyridine ligand were connected with an alkyl chain (Figure 2a). The bipyridine C4, where the substituent does not hinder osmium complexation,[7c] was linked to the 6-amino group of adenine, which is a modifiable functional group locating in the DNA major groove. The best-suited length of the alkyl linker was determined by molecular modeling. The linker end of a ligand 6-(4′-methyl-2,2′-bipyridine-4-yl)hexanoic acid[7c] was converted into an amino group to yield **1** (85%), followed by a nucleophilic attack of **1** on 6-chloropurine 2′-deoxyriboside to yield **2** (95%) (Scheme 2). The resulting bipyridine-tethered nucleoside "B" was incorporated into a DNA strand by a conventional method using a phosphoramidite form **3**. We prepared a 20-nucleotide fragment of the *p53* gene exon 5 containing a methylation hot spot as the target strand (Figure 2b, DNA2(N))[9] and synthesized an artificial DNA designed so that a B base was positioned opposite the target methylated/unmethylated cytosine, 5′-d(TGTGAGGCBCTGCCCCCACC)-3′ (DNA2′). The reaction mixture was incubated at 50 °C for a period of 10 min. Reaction of ^{32}P-labeled DNA2(C) was not observed in the mixture containing DNA2′ (lane 7), similar to the results for mixtures lacking either potassium osmate(VI) or DNA2′ (lanes 1−6). Conversely, the reaction of ^{32}P-labeled DNA2(M) in the presence of both potassium osmate(VI) and DNA2′ produced a product with a higher molecular weight, which appeared as a band of low mobility on PAGE (Figure 2b (i), lane 8). Treatment of the reaction product with hot piperidine eliminated the high-molecular-weight band and produced a new band that indicated cleavage of the strand at the 5-methylcytosine (Figure 2b (ii), lane 8). The appearance of this new band suggests that an interstrand cross-link, mediated by osmium complexation,

(8) (a) Hunter, W. N.; Brown, T.; Anand, N. K.; Kennard, O. *Nature* **1986**, *320*, 552−555. (b) Hunter, W. N.; Brown, T.; Kennard, O. *Nucleic Acids Res.* **1987**, *15*, 6589−6606. (c) Kalnik, M. W.; Kouchakdjian, M.; Li, B. F. L.; Swann, P. F.; Patel, D. J. *Biochemistry* **1988**, *27*, 100−108. (d) Okamoto, A.; Tanaka, K.; Saito, I. *J. Am. Chem. Soc.* **2004**, *126*, 9458−9463.

(9) (a) Tornaletti, S.; Pfeifer, G. P. *Oncogene* **1995**, *10*, 1493−1499. (b) Greenblatt, M. S.; Bennett, W. P.; Hollstein, M.; Harris C. C. *Cancer Res.* **1994**, *54*, 4855−4878.

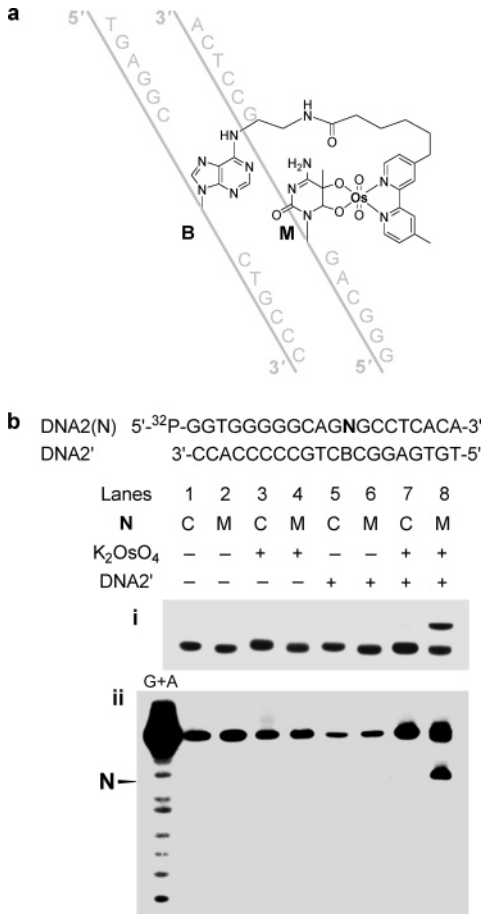

Figure 2. Interstrand cross-linking mediated by osmium complexation between 5-methylcytosine and a bipyridine-tethered adenine derivative. (a) Structure of an osmium complex between 5-methylcytosine and a newly designed bipyridine-tethered nucleoside, B. (b) Interstrand cross-link formation. (i) PAGE analysis of the samples after osmium complexation; (ii) PAGE analysis after hot piperidine treatment of the samples shown in (i).

occurred between DNA2(M) and DNA2′. The mass spectrometric data for the product generated after osmium complexation with DNA2(M)/DNA2′ directly indicate the production of a cross-linked adduct ($[M + H]^+$, calcd 9690.79, found 9688.31). The effect of the cross-link formation was also reflected in the thermal stability of the duplex. The melting temperature (T_m) of the duplex DNA2(M)/DNA2′ in 50 mM sodium phosphate (pH = 7.0) and 100 mM sodium chloride was 55 °C before complexation (black dots in Figure 3), whereas the T_m value after complexation was >80 °C (red dots). Thus, the osmium complex was stable to heating. It was also determined by HPLC analysis that there was no degradation of the cross-linked structure during incubation at 90 °C for 24 h.

Application to Methylation Analysis: Model Experiments. These interstrand complexes formed by osmium and nucleic acids (ICON) should allow sequence-selective labeling and the obstruction of PCR amplification at the target 5-methylcytosine. The sequence-selective distinction of unmethylated and methylated cytosines is significant for studies of epigenetic mechanisms because methylation plays crucial roles in the regulation of chromatin stability,[10] gene deactivation,[11] parental imprinting,[12] and carcinogenesis.[13] Conventional techniques for methylation detection can be divided roughly into two types: DNA fragmentation by restriction enzymes[14] and cytosine deamination by bisulfite salt.[15] In the former method, the CpG methylation-sensitive restriction endonucleases have been used to survey the extent of DNA methylation. The available target sequences are limited, and comparatively large amounts of genomic samples are required. In the latter method, the deamination of unmethylated cytosines is mainly caused by the bisulfite salt; that is, sodium bisulfite is used to convert cytosine residues into uracil residues in single-stranded DNA, under conditions whereby 5-methylcytosine remains "nonreactive". Although the sequence information is amplified by PCR after bisulfite treatment, the long-term reaction causes serious damage to the original sequence information by depyrimidination (the strand that has not suffered damage falls below 0.1% with 16 h incubation for strand lengths of 100 nucleotides).[16] The establishment of methylation-typing techniques based on other concepts is necessary to elucidate the role of each methylation to proceed to the next stage of the present research involving rough scanning and scoring the methylcytosines in genes. The key points required for a newly designed assay for methylation typing are as follows: (1) sequence selectivity, (2) quantitative analysis, (3) shorter reaction times, (4) less sample damage, and (5) need for a smaller amount of genomic sample. The concept of sequence-specific ICON has the capacity to meet these criteria.

To construct a prototype for ICON-based methylation analysis, we designed a model methylcytosine-typing experiment. We prepared a fragment of the tumor suppressor *retinoblastoma* (*RB1*) gene exon 8 (59639−59730) containing two methylation

(10) (a) Robertson, K. D. *Oncogene* **2002**, *21*, 5361−5379. (b) Miura, A.; Yonebayashi, S.; Watanabe, K.; Toyama, T.; Shimada, H.; Kakutani, T. *Nature* **2001**, *411*, 212−214. (c) Jones, P. L.; Wolffe, A. P. S. *Cancer Biol.* **1999**, *9*, 339−347. (d) Pogribny I. P.; Basnakian, A. G.; Miller, B. J.; Lopatina, N. G.; Poirier, L. A.; James, S. J. *Cancer Res.* **1995**, *55*, 1894−1901.

(11) (a) Tate, P. H.; Bird, A.P. *Curr. Opin. Genet. Dev.* **1993**, *3*, 226−231. (b) Colot, V.; Rossignol, J. L. *BioEssays* **1999**, *21*, 402−411. (c) Feil, R.; Khosla, S. *Trends Genet.* **1999**, *15*, 431−435. (d) Bird, A. *Genes Dev.* **2002**, *16*, 6−21.

(12) (a) Hata, K.; Okano, M.; Lei, H.; Li, E. *Development* **2002**, *129*, 1983−1993. (b) Howell, C. Y.; Bestor, T. H.; Ding, F.; Latham, K. E.; Mertineit, C.; Trasler, J. M.; Chaillet, J. R. *Cell* **2001**, *104*, 829−838. (c) Constancia, M.; Pickard, B.; Kelsey, G.; Reik, W. *Genome Res.* **1998**, *8*, 881−900. (d) Wutz, A.; Smrzka, O. W.; Schweifer, N.; Schellander, K.; Wagner, E. F.; Barlow, D. P. *Nature* **1997**, *389*, 745−749. (e) Li, E.; Beard, C.; Jaenisch, R. *Nature* **1993**, *366*, 362−365.

(13) (a) Kanaya, T.; Kyo, S.; Maida, Y.; Yatabe, N.; Tanaka, M.; Nakamura, M.; Inoue, M. *Oncogene* **2003**, *22*, 2352−2360. (b) Kanyama, Y.; Hibi, K.; Nakayama, H.; Kodera, Y.; Ito, K.; Akiyama, S.; Nakao, A. *Cancer Sci.* **2003**, *94*, 418−420. (c) Toyota, M.; Sasaki, Y.; Satoh, A.; Ogi, K.; Kikuchi, T.; Suzuki, H.; Mita, H.; Tanaka, N.; Itoh, F.; Issa, J.-P. J.; Jair, K.-W.; Schebel, K. E.; Imai, K. *Proc. Natl. Acad. Sci. U.S.A.* **2003**, *100*, 7818−7823. (d) Karpf, A. R.; Jones, D. A. *Oncogene* **2002**, *21*, 5496−5503. (e) Robertson, K. D.; Jones, P. A. *Carcinogenesis* **2000**, *21*, 461−467. (f) Schmutte, C.; Jones, P. A. *Biol. Chem.* **1998**, *379*, 377−388.

(14) (a) Kane, M. F.; Loda, M.; Gaida, G. M.; Lipman, J.; Mishra, R.; Goldman, H.; Jessup, J. M.; Kolodner, R. *Cancer Res.* **1997**, *57*, 808−811. (b) Okamoto, A.; Tanabe, K.; Saito, I. *J. Am. Chem. Soc.* **2002**, *124*, 10262−10263. (c) Okamoto, A. *Bull. Chem. Soc. Jpn.* **2005**, *78*, 2083−2097. (d) Nelson, P. S.; Papas, T. S.; Schweinfest, C. W. *Nucleic Acids Res.* **1993**, *21*, 681−686. (e) Tasserondejong, J. G.; Aker, J.; Giphartgassler, M. *Gene* **1988**, *74*, 147−149. (f) Butkus, V.; Petrauskiene, L.; Maneliene, Z.; Klimasauskas, S.; Laucys, V.; Janulaitis, A. *Nucleic Acids Res.* **1987**, *15*, 7091−7102.

(15) (a) Hayatsu, H.; Wataya, Y.; Kai, K.; Iida, S. *Biochemistry* **1970**, *9*, 2858−2866. (b) Gonzalgo, M. L.; Jones, P. A. *Nucleic Acids Res.* **1997**, *25*, 2529−2531. (c) Herman, J. G.; Graff, J. R.; Myöhänen, S.; Nelkin, B. D.; Baylin, S. B. *Proc. Natl. Acad. Sci. U.S.A.* **1996**, *93*, 9821−9826. (d) Clark, S. J.; Harrison, J.; Paul, C. L.; Frommer, M. *Nucleic Acids Res.* **1994**, *22*, 2990−2997. (e) Frommer, M.; McDonald, L. E.; Millar, D. S.; Collis, C. M.; Watt, F.; Grigg, G. W.; Molloy, P. L.; Paul, C. L. *Proc. Natl. Acad. Sci. U.S.A.* **1992**, *89*, 1827−1831. (f) Warnecke, P. M.; Stirzaker, C.; Song, J.; Grunau, C.; Melki, J. R.; Clark, S. J. *Methods* **2002**, *27*, 101−107.

(16) (a) Tanaka, K.; Okamoto, A. *Bioorg. Med. Chem. Lett.* **2007**, *17*, 1912−1915. (b) Raizis, A. M.; Schmitt, F.; Jost, J.-P. *Anal. Biochem.* **1995**, *226*, 161−166.

Scheme 2. Synthesis of a Bipyridine-Modified Adenine Derivative

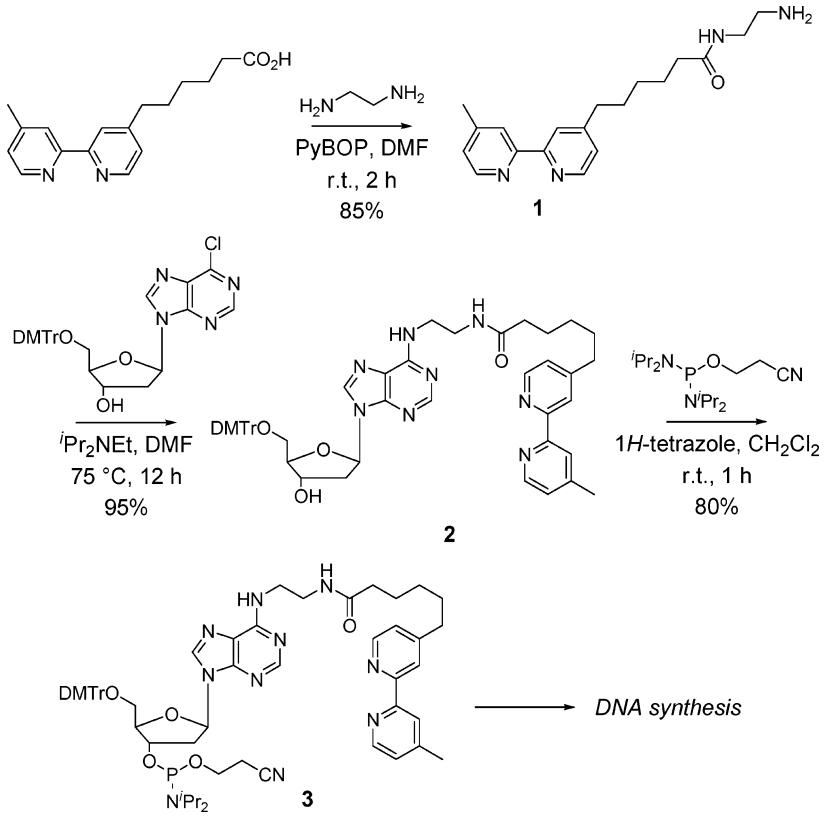

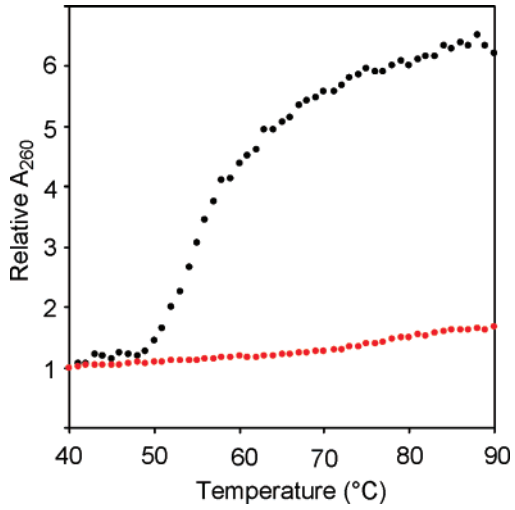

Figure 3. Measurements of the melting temperatures (T_m) of DNA2(M)/DNA2′. The T_m of the duplex (2.5 μM) before/after osmium complexation was measured in 50 mM sodium phosphate buffer (pH 7.0) containing 100 mM sodium chloride. Black, before complexation; red, after complexation. Absorbance versus temperature profiles were measured at 260 nm.

hot spots at codon 251 (59683/4) and codon 255 (59695/6) (Figure 4).[17] Two B-incorporated DNAs were designed for one methylation target, which hybridized with the sense and antisense strands, and their sequences were chosen to avoid tight hybridization between the B-incorporated DNAs themselves. A solution of the target duplex and the bipyridine-labeled DNAs containing all the reaction reagents except potassium osmate(VI) was heated at 95 °C for 5 min to cause denaturation and immediately cooled to 0 °C. Then, potassium osmate(VI) was added, and the mixture was incubated at 55 °C for 60 min. The reaction sample was filtered for deionization and amplified using real-time PCR. The methylation status of the target cytosine was determined from the increase in the SYBR Green I fluorescent signal associated with the exponential growth of the PCR product. Amplification of the unmethylated DNA started first, and then the amplification of the methylated DNA started several cycles later (Figure 5a). The ICON at the methylation site brought about this lag in the starting point of amplification. The amplification curves for the methylated duplexes almost overlapped those for a 0.1 concentration of the unmethylated duplexes, suggesting that the PCR-blocking efficiency of ICON was approximately 90%. The second derivative maximum of the amplification curves, as an index for the amplification starting point, exhibited a linear dependence on the logarithm of the methylated duplex concentration (Figure 5b). The proportion of methylation was also quantifiable in a similar manner. A linear relationship between the amplification starting point and the logarithm of the methylation proportion allowed the calculation of the proportion of methylation at the target cytosine (Figure 5c). An ICON with B-containing DNAs designed for each target cytosine occurred easily depending on the amount of the DNA methylated at the target cytosine and was completely independent of the amount of other methylated DNA (Figure 5d). Blocking of PCR by ICON at the methylation site made possible the sequence-specific quantification of methylation.

Application to Methylation Analysis: The Mouse Genome. The sequence-specific ICON was used to quantify the methylation of the mouse genome, which was collected from four different tissues, kidney, liver, spleen, and testis. Two CpG

(17) Mancini, D.; Singh, S.; Ainsworth, P.; Rodenhiser, D. *Am. J. Hum. Genet.* **1997**, *61*, 80−87.

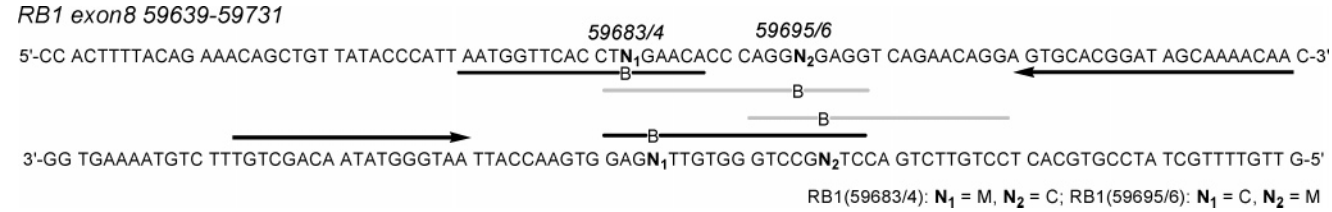

Figure 4. Sequence design for sequence-specific methylation quantification model experiments. Arrows indicate the primer binding sites. Black lines show B-containing DNA probes for the 59683/4 methylation site. Gray lines show B-containing DNA probes for the 59695/6 methylation site. Details of the sequences of primers and probes are given in the Experimental Section.

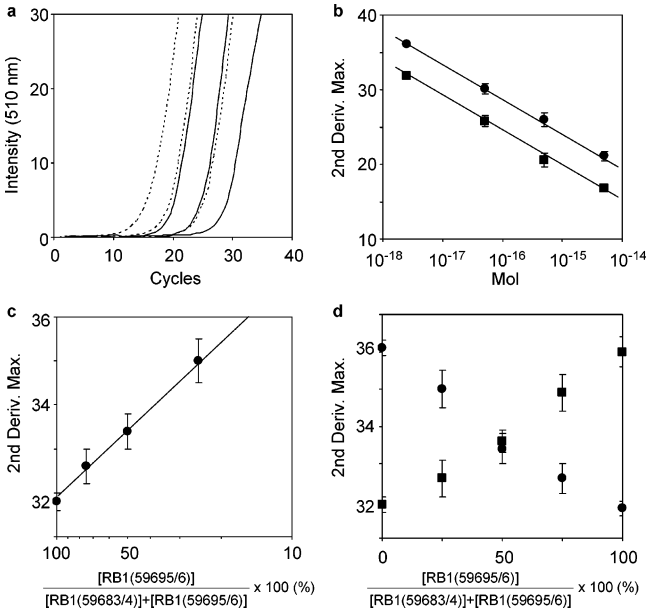

Figure 5. Model experiments for sequence-specific methylation quantification. (a) Typical amplification curves. Probes for 59683/4 detection (black lines for N_1 in Figure 4) were used for different concentrations of RB1-(59683/4) (solid lines) or RB1(59685/6) (dotted lines). The amounts of the starting DNA duplexes are 5.0×10^{-15}, 5.0×10^{-16}, and 5.0×10^{-17} mol. (b) Relationship between starting DNA duplex concentration and amplification starting point. Probes for 59683/4 (N_1) detection (black lines in Figure 4) were used for different concentrations of RB1(59683/4) (circles) or RB1(59695/6) (squares). The amounts of the starting DNA duplexes are 5.0×10^{-15}, 5.0×10^{-16}, 5.0×10^{-17}, and 2.5×10^{-18} mol. The *y*-axis shows the second derivative maxima of the amplification curves. The means ± standard deviations of five independent experiments are presented. (c) Linear relationship between the methylation proportion and the amplification starting point in the experiments using the 59683/4 probes (black lines in Figure 4). The *y*-axis shows the second derivative maxima of the amplification curves. Presented are mean ± standard deviations from five independent experiments. (d) Relationship between the proportion of methylation and the amplification starting point. A sample including a mixture of RB1(59683/4) and RB1(59695/6) in different proportions was used in the presence of the probe for either 59683/4 (circles, black lines in Figure 4) or 59695/6 (squares, gray lines in Figure 4). The means ± standard deviations of five independent experiments are presented.

sequences (chromosome 11, #115,285,676 and #115,285,805) in a tissue-specifically differentially methylated region were chosen as the targets, and four B-labeled DNAs were designed for these targets. A 60 min incubation and a 90 min PCR analysis were performed with 20 ng of the mouse genome. Samples from different tissues exhibited characteristic methylation levels for the two methylation sites (Table 1). These data agree closely with the degree of methylation quantified by mass spectrometric analysis of fragmented and bisulfite-treated genome samples.[18]

Table 1. Methylation Analysis of the Mouse Genome[a]

		ICON		Bisulfite Mass Spec[b]	
		115,285,676	115,285,805	115,285,676	115,285,805
1	testis	8 (7)	4 (4)	24	8
2	kidney	96 (5)	91 (5)	93	83
3	spleen	91 (8)	95 (15)	97	100
4	liver	95 (4)	69 (5)	95	45

[a] The unit is %. Numbers in parentheses are standard deviation from five independent experiments. [b] Data from ref 18.

Conclusions

We have described a new, high value aspect of osmium−DNA complexation. The discovery of this efficient osmium complexation reactivity for the 5-methylcytosine−adenine-mismatched base pair enabled the design of a functional nucleoside for sequence-specific DNA methylation analysis. The connection between an adenine base of a short DNA forming a 5-methylcytosine−adenine-mismatched base pair by hybridization and a bipyridine group required for osmium-centered complex formation results in the complexation at a specific 5-methylcytosine regardless of other reactive 5-methylcytosine and thymine bases in a long DNA strand. Although there still remain further aspects to be examined toward an easier-to-use methylation analysis, such as further improvement of the reaction yield for osmium complexation at 5-methylcytosine and optimization of PCR conditions suitable for ICON, we anticipate that this new concept of sequence-specific short-term methylation analysis supported by the chemical basis will be the starting point for an epoch-making methylation-typing assay, which will supersede conventional methods.

Experimental Section

***N*-(2-Aminoethyl) (4′-methyl-2,2′-bipyridin-4-yl)hexanamide (1).** A mixture of (4′-methyl-2,2′-bipyridin-4-yl)hexanoic acid (568 mg, 2.0 mmol) and PyBOP (1.14 g, 2.2 mmol) in DMF (10 mL) was stirred at room temperature for 30 min. To the solution was added ethylenediamine (222 μL, 2.2 mmol), and the mixture was stirred at room temperature for 2 h. The resulting mixture was concentrated in vacuo and diluted with chloroform. The organic phase was washed with 1 N NaOH and brine, dried over $MgSO_4$, and concentrated in vacuo to yield **1** (603 mg, 1.7 mmol, 85%) as a brown oil: ^{1}H NMR (400 MHz, $CDCl_3$) δ 8.46 (t, 2H, J = 5.4 Hz), 8.20 (d, 2H, J = 6.8 Hz), 7.12−7.08 (m, 2H), 2.66 (quartet, 2H, J = 7.8 Hz), 2.42 (s, 3H), 2.20−2.12 (m, 2H), 1.72−1.52 (m, 4H), 1.42−1.39 (m, 4H), 1.32−1.25 (m, 2H); ^{13}C NMR (100 MHz, $CDCl_3$) δ 155.9, 152.4, 148.8, 148.7, 148.0, 124.5, 123.8, 121.9, 121.1, 38.8, 36.2, 35.1, 29.9, 28.7, 26.7, 20.1; FABMS (NBA/$CHCl_3$) m/z 327 ([(M + H)$^+$]), HRMS calcd for $C_{19}H_{27}ON_4$ ([(M + H)$^+$]) 327.2185, found 327.2184.

(18) Kitamura, E.; Igarashi, J.; Morohashi, A.; Hida, N.; Oinuma, T.; Nemoto, N.; Song, F.; Ghosh, S.; Held, W. A.; Yoshida-Noro, C.; Nagase, H. *Genomics* **2007**, *89*, 326−327.

(6-(2-(6-(4′-Methyl-2,2′-bipyridin-4-yl)hexanamido)ethylamino)-9*H*-purin-9-yl)-5′-*O*-dimethoxytrityl-2′-deoxyriboside (2). To a solution of (6-chloro-9*H*-purin-9-yl)-5′-*O*-dimethoxytrityl-2′-deoxyriboside (11.0 g, 19.2 mmol) in DMF (50 mL) were added diisopropylethylamine (23 mL) and **1** (18.1 g, 55.4 mmol) in DMF (50 mL) at room temperature, and the mixture was stirred at 75 °C for 12 h. After diluted with ethyl acetate (1 L), the resulting mixture was washed with brine, dried over Na_2SO_4, filtered, and evaporated under reduced pressure. The crude product was purified by silica gel column chromatography (chloroform/methanol = 50:1 containing 1% NH_4OH) to yield **2** (15.8 g, 18.3 mmol, 95%) as a white solid: ^{1}H NMR (400 MHz, CD_3OD) δ 8.41 (dd, 2H, J = 4.8, 10.1 Hz), 8.17 (s, 1H), 8.12 (s, 1H), 8.04 (s, 2H), 7.33 (d, 2H, J = 7.3 Hz), 7.20 (d, 4H, J = 8.8 Hz), 7.15−7.08 (m, 5H), 6.71 (dd, 4H, J = 4.0, 8.4 Hz), 6.38 (t, 1H, J = 6.2 Hz), 4.60 (quartet, 1H, J = 4.2 Hz), 4.10 (quartet, 1H, J = 4.4 Hz), 3.66 (s, 6H), 3.43 (t, 2H, J = 5.9 Hz), 3.32−3.27 (m, 2H), 2.83 (dt, 1H, J = 6.2, 13.5 Hz), 2.56 (t, 2H, J = 7.5 Hz), 2.44 (ddd, 1H, J = 4.6, 6.2, 13.4 Hz), 2.36 (s, 3H), 2.11 (t, 2H, J = 7.1 Hz), 1.61−1.50 (m, 4H), 1.29−1.23 (m, 2H); ^{13}C NMR (100 MHz, CD_3OD) δ 176.3 160.0, 157.0, 156.3, 154.7, 153.8, 150.3, 150.0, 149.9, 146.2, 140.4, 137.10, 137.06, 131.23, 131.20, 129.3, 128.7, 127.8, 126.0, 125.4, 123.6, 122.9, 114.0, 87.9, 87.6, 85.8, 72.6, 65.0, 55.7, 40.8, 40.3, 36.9, 36.0, 30.9, 29.6, 26.5, 21.2; FABMS (NBA/CH_3OH) m/z 863 ([(M + H)$^+$]), HRMS calcd for $C_{50}H_{55}O_6N_8$ ([(M + H)$^+$]) 863.4245, found 863.4235.

5′-*O*-Dimethoxytrityl-6-*N*-[9-(4′-methyl-2,2′-bipyridin-4-yl)-3-oxa-2-azanonyl]-2′-deoxyadenine 3′-(2-cyanoethyl *N*,*N*-diisopropylphosphoramidite) (3). To a solution of **2** (432 mg, 0.5 mmol) and 1*H*-tetrazole (35 mg, 0.5 mmol) in anhydrous dichloromethane (2.5 mL) was added 2-cyanoethyl tetraisopropylphosphorodiamidite (151 mg, 0.6 mmol) under nitrogen. The mixture was stirred at room temperature. After stirring for 1 h, the reaction mixture was diluted with dichloromethane (50 mL) and then washed with saturated sodium bicarbonate solution (50 mL × 2). An aqueous layer was back extracted by dichloromethane (50 mL). Combined organic layer was dried with sodium sulfate and then evaporated. The crude mixture was dissolved in ethyl acetate and reprecipitated into hexane. Precipitate was filtrated and redissolved in dry acetonitrile then evaporated in vacuo to yield **3** (two diastereomeric isomers) as a pale yellow foam (420 mg, 80%). The product was used for conventional solid-phase DNA synthesis without further purification: ^{31}P NMR (160 MHz, $CDCl_3$) δ 149.39, 149.28; FAB HRMS (NBA) m/z calcd for $C_{59}H_{72}N_{10}O_7P$ ([(M + H)$^+$]) 1063.5318, found 1063.5292.

DNA Synthesis and Characterization. Artificial DNA was synthesized by the conventional phosphoramidite method by using an Applied Biosystems 392 DNA/RNA synthesizer. Synthesized DNA was purified by reverse phase HPLC on a 5-ODS-H column (10 × 150 mm, elution with a solvent mixture of 0.1 M triethylammonium acetate (TEAA), pH 7.0, linear gradient over 30 min from 5 to 20% acetonitrile at a flow rate 3.0 mL/min). Each ODN was characterized by MALDI-TOF MS. DNA2′, 5′-d(TGTGAGGCBCTGCCCCCACC)-3′ ([M − H]$^-$, calcd 6347.30, found 6347.96). Probes for RB1 59683/4 methylation site, 5′-d(TGTTCBAGGTGAACCATTp)-3′ ([M − H]$^-$, calcd 5901.97, found 5901.61), 5′-d(CTCBAACACCCAGGCGAGp)-3′ ([M − H]$^-$, calcd 5850.94, found 5849.51). Probes for RB1 59695/6 methylation site, 5′-d(AGGCBAGGTCAGAACAGGp)-3′ ([M − H]$^-$, calcd 5995.04, found 5994.40), 5′-d(CCTCBCCTGGGTGTTCGAp)-3′ ([M − H]$^-$, calcd 5854.91, found 5854.81). Probes for mouse chr11 115,285,676 methylation site, 5′-d(GCTCBGGGACCTCGTTGGp)-3′ ([M − H]$^-$, calcd 5919.94, found 5919.37), 5′-d(CCCCBAGCCCAAAGAGGAp)-3′ ([M − H]$^-$, calcd 5859.96, found 5859.39). Probes for mouse chr11 115,285,805 methylation site, 5′-d(ATACBTCACGGGCGTGACp)-3′ ([M − H]$^-$, calcd 5896.96, found 5895.37), 5′-d(TGACBTATATGCAGAAGCp)-3′ ([M − H]$^-$, calcd 5920.00, found 5919.29).

Preparation of ^{32}P-5′-End-Labeled DNA. The DNAs (400 pmol strand) were 5′-end-labeled by phosphorylation with 4 μL of [γ-^{32}P]-ATP (Amersham) and T4 polynucleotide kinase using a standard procedure. The 5′-end-labeled DNA was recovered by ethanol precipitation and further purified by 15% denaturing polyacrylamide gel electrophoresis (PAGE).

Osmium Oxidation of ^{32}P-5′-End-Labeled DNA (Bipyridine Use). The 5′-end-labeled DNA1(N) (10 pmol strand) to be examined was incubated in a solution of 1 μM DNA1′(N′), 5 mM potassium osmate, 100 mM potassium hexacyanoferrate(III), 100 mM bipyridine, and 1 mM EDTA in 100 mM Tris-HCl buffer (pH 7.7) and 10% acetonitrile at 0 °C for 5 min. The reaction mixture was ethanol precipitated with the addition of 15 μL of 3 M sodium acetate (pH 5.0), 10 μL of salmon sperm DNA (1 mg/mL), and 1 mL of cold ethanol. The precipitated DNA was washed with 150 μL of 80% cold ethanol and dried in vacuo. The precipitated DNA was redissolved in 50 μL of 10% piperidine (v/v), heated at 90 °C for 20 min, and then evaporated to dryness by vacuum rotary evaporation.

Osmium Oxidation of ^{32}P-5′-End-Labeled DNA (B-Containing DNA Use). The 5′-end-labeled DNA2(N) (10 pmol strand) to be examined was incubated in a solution of 1 μM DNA2′, 5 mM potassium osmate, 100 mM potassium hexacyanoferrate(III), and 1 mM EDTA in 100 mM Tris-HCl buffer (pH 7.0) and 10% acetonitrile at 50 °C for 10 min. The reaction mixture was ethanol precipitated with the addition of 15 μL of 3 M sodium acetate (pH 5.0), 10 μL of salmon sperm DNA (1 mg/mL), and 1 mL of cold ethanol. The precipitated DNA was washed with 150 μL of 80% cold ethanol and dried in vacuo. For determination of the reaction site, the precipitated DNA was redissolved in 50 μL of 10% piperidine (v/v), heated at 90 °C for 20 min, and then evaporated to dryness by vacuum rotary evaporation.

Polyacrylamide Electrophoresis of Reaction Samples. The dried-up reaction sample was resuspended in 5−20 μL of 80% formamide loading buffer (a solution of 80% formamide (v/v), 1 mM EDTA, 0.1% xylenecyanol, and 0.1% bromophenol blue). The samples (1 μL, 3−10 kcpm) were loaded onto 15% denaturing 19:1 acrylamide/bisacrylamide gel containing 7 M urea, electrophoresced at 1900 V for approximately 1 h, and transferred to a cassette and stored at −80 °C with X-ray film.

Melting Temperature (T_m) Measurements. All T_m measurements of the DNA duplexes (2.5 μM, final duplex concentration) were made in 50 mM sodium phosphate buffer (pH 7.0) containing 100 mM sodium chloride. Absorbance versus temperature profiles were measured at 260 nm with a Shimadzu UV-2550 spectrophotometer equipped with a Peltier temperature controller using a cell with a 1 cm path length. The absorbance of the samples was monitored at 260 nm from 5 to 90 °C, with a heating rate of 1 °C/min. From these profiles, first derivatives were calculated to determine T_m values.

Sequences of ICON Probes and PCR Primers in Methylation Quantification Experiments. *For model RB1 study*. Probes for site 59683/4, 5′-d(TGTTCBAGGTGAACCATTp)-3′ and 5′-d(CTCBAACACCCAGGCGAGp)-3′. Probes for site 59695/6, 5′-d(AGGCBAGGTCAGAACAGGp)-3′ and 5′-d(CCTCBCCTGGGTGTTCGAp)-3′. Primers, 5′-d(ACAGCTGTTATACCCATT)-3′ and 5′-d(GTTGTTTTGCTATCCGTGCA)-3′. *For mouse genome study*. Probes for chr11 115,285,676, 5′-d(GCTCBGGGACCTCGTTGGp)-3′ and 5′-d(CCCCBAGCCCAAAGAGGAp)-3′. Probes for chr11 115,285,805, 5′-d(ATACBTCACGGGCGTGACp)-3′ and 5′-d(TGACBTATATGCAGAAGCp)-3′. Primers, 5′-d(GGAGCCTGCTGAGGCCTGT)-3′ and 5′-d(CAGTGCAAAACCCAGGTTCA)-3′; "p" is a phosphate group of the 3′ end to avoid that probes work as PCR primers.

Methylation Quantification. The model DNA duplex (100 nM or the desired concentration) or genome DNA (20 ng) was added into a solution (16 μL) of B-containing DNA probes (1 nM each for the sense and antisense strands), 100 mM potassium hexacyanoferrate(III), 0.5 mM EDTA, and 1 M sodium chloride in 50 mM Tris-HCl buffer (pH 7.7). The reaction mixture was incubated at 95 °C for 5 min and then cooled to 0 °C immediately. To the mixture was added 25 mM potassium osmate (4 μL), and the reaction was allowed to proceed at

55 °C for 60 min. The reaction solution was filtered to deionize it. The process of PCR amplification was performed in a reaction solution of DNA, 0.6 U *TaKaRa Ex Taq*, 10× buffer, 2.5 mM dNTP mix, 10 mM primer mix, and SYBR Green I. Amplifications were performed in tubes as follows: 50 cycles of denaturation at 95 °C for 5 s, annealing with fluorescence monitoring at 60 °C for 10 s, and extension at 72 °C for 15 s on the Corbett Rotor-Gene. The amplification process was monitored by the fluorescence of SYBR Green I (470 nm/510 nm). The second derivative of the amplification plot produces peaks corresponding to the maximum rate of fluorescence increase in the reaction. The amount of methylation was calculated from the value of the second derivative of each sample using a calibration curve acquired by the data from the standard samples.

Acknowledgment. We thank Prof. H. Nagase at Nihon University for the gift of mouse genome and helpful discussion (supported by Nihon University Multidisciplinary Research Grant for 2006 and the Academic Frontier Project for 2006 Project for Private Universities, a matching fund subsidy from MEXT). This work was supported by Industrial Technology Research Grant Program in 2006 from New Energy and Industrial Technology Development Organization (NEDO) of Japan. (to A.O.).

JA076140R